Data-Driven Decentralized Resilient Control for Large-Scale Systems Under DoS Attacks

Lijuan Zha, Jinzhao Miao, Jinliang Liu, *Senior Member, IEEE*, Engang Tian, *Senior Member, IEEE*, and Chen Peng, *Senior Member, IEEE*

***Abstract*—This paper investigates the data-driven decentralized resilient control problem for large-scale systems (LSS) under randomly occurring Denial-of-Service (DoS) attacks. A min-max optimization criterion is established based on zero-sum differential game theory, and the corresponding optimal control strategy is derived. Global asymptotic stability of the closed-loop LSS is theoretically guaranteed under the proposed control scheme. A two-stage adaptive dynamic programming (ADP) algorithm, integrating reinforcement learning techniques with local state feedback, is proposed to derive the optimal control policy without requiring prior knowledge of the system model. Simulations are conducted in MATLAB on a multimachine power system benchmark. In particular, the two-stage ADP controller shortens the settling time by up to 7.7% and reduces overshooting by over 14.5% compared to the existing methods, thereby validating its robustness and superior performance in dynamic and adversarial environments.**

***Index Terms*—Large-scale systems, decentralized control, data-driven, DoS attacks.**

I. Introduction

LARGE-SCALE systems (LSS) are complex, interconnected networks composed of dynamically interacting subsystems that are often distributed across broad geographical regions [1]. These systems are characterized by high dimensionality, intricate interdependencies, and decentralized architectures [2], where each subsystem operates with local control and communicates with limited neighboring nodes [3]. Classic examples of large-scale systems (LSS) include smart grids, transportation systems, urban water networks, and multi-agent robotic platforms [4]. With the rapid evolution of smart technologies, the domain of LSS has begun to extend into Internet of Things (IoT) ecosystems, particularly within consumer electronics. A notable and emerging application is the integration of holographic counterparts in IoT-based consumer technologies [5]. This development encompasses immersive user interfaces, such as holographic displays, augmented reality wearables, and intelligent home environments [6], which require large-scale coordination among distributed sensors, actuators, and edge computing units to support seamless, real-time interactions [7]. In these applications, ensuring responsive, stable, and robust performance under uncertainties and attack threats is especially critical. Furthermore, as LSS increasingly rely on wireless communication and networked computing, they become more susceptible to a broad range of cyber threats.

Effectively addressing these challenges is vital not only for the protection of national infrastructure but also for enabling the next generation of intelligent, sustainable, and consumer-centric systems. Nowadays, decentralized control has emerged as a key solution for LSS [8]. In contrast to centralized methods that depend on a global controller, decentralized approaches use locally situated controllers that operate with limited communication and partial information [9], which are more scalable and resilient for complex systems with delays and computational constraints [10]. Recent advancements in this field have demonstrated the feasibility of applying decentralized and robust control strategies to practical scenarios, including immersive IoT consumer platforms with holographic interfaces, distributed renewable energy management, and autonomous mobility systems [11]. These developments highlight the growing relevance and application of LSS control theory in consumer technology driven by holographic and interactive innovations. In [12], a novel local value function was constructed to eliminate unmatched interconnections with unknown time delays, addressing the problem of decentralized optimal control for LSS with unknown delays. In [13], a cyclic small-gain technique was introduced to resolve the issue of unmatched interconnections in LSS, and a decentralized fault-tolerant control method was proposed for a class of LSS with actuator failures. These efforts aim to enhance the scalability, robustness, and efficiency of LSS by leveraging local information and minimizing communication requirements [14]. Despite these advancements, challenges remain, particularly in ensuring stability and performance under dynamic environments and cyber threats.

Received 14 January 2025; revised 10 April 2025 and 22 May 2025; accepted 1 June 2025. Date of publication 5 June 2025; date of current version 14 August 2025. This work was supported in part by the National Natural Science Foundation of China under Grant 62273174, Grant 62373252, and Grant 62441310; in part by the Natural Science Foundation of Jiangsu Province of China under Grant BK20230063; and in part by the Startup Foundation for Introducing Talent of NUIST under Grant 2024r063. *(Corresponding author: Jinliang Liu.)*

Lijuan Zha is with the School of Science, Nanjing Forestry University, Nanjing 210037, China (e-mail: zhalijuan@vip.163.com).

Jinzhao Miao and Jinliang Liu are with the School of Computer Science, Nanjing University of Information Science and Technology, Nanjing 210044, China (e-mail: miaojinzhao2022@163.com; liujinliang@vip.163.com).

Engang Tian is with the School of Optical-Electrical and Computer Engineering, University of Shanghai for Science and Technology, Shanghai 200093, China (e-mail: tianengang@163.com).

Chen Peng is with the School of Mechatronic Engineering and Automation, Department of Automation, Shanghai University, Shanghai 200444, China (e-mail: c.peng@shu.edu.cn).

Digital Object Identifier 10.1109/TCE.2025.3576804

Cyber-attacks pose significant threats to modern control systems, particularly as these systems increasingly rely on interconnected networks for communication and operation [15]. Various forms of cyber attacks, including deception attacks [16], replay attacks, eavesdropping [17], and Denial-of-Service (DoS) attacks [18], target the integrity, confidentiality, and availability of system resources [19]. Among various types of cyberattacks, DoS attacks have emerged as a particularly critical threat in networked control systems due to their simplicity in execution and potential for widespread disruption [20]. Unlike other cyber threats that often require sophisticated intrusion strategies or stealth, DoS attacks exploit system vulnerabilities through high-volume traffic flooding or targeted interference [21], making them easier to launch but challenging to defend against, especially in distributed and heterogeneous environments [22]. Such attacks can cause delayed, corrupted, or lost data, resulting in degraded control and potential system instability [23]. Therefore, mitigating DoS attack risks is a key focus in secure control research. To mitigate the adverse effects of potential DoS attacks in LSS, in [24], a compensator was designed to estimate unmeasurable state variables, and an adaptive decentralized secure control method for nonlinear LSS was developed. To reduce computational burdens and resist DoS attacks, in [25], a distributed sampled-data resilient control strategy for multi-agent systems was proposed. In [26], a distributed event-triggered control method was introduced for multifunctional grid-connected inverters in microgrids to enhance power quality under DoS attacks. However, most existing approaches focus on small to medium scale systems, with limited scalability and adaptability to the high-dimensional, interdependent nature of LSS. These limitations highlight the urgent need for innovative control strategies tailored to LSS.

Data-driven approaches have emerged as powerful tools for solving control problems in complex systems, particularly when system dynamics are partially unknown or difficult to model explicitly [27]. Among these methods, adaptive dynamic programming (ADP) has gained significant attention for its ability to approximate optimal control policies using system data [28]. ADP leverages the principles of optimal control to iteratively improve performance by learning from system interactions [29]. In recent years, extensive research has been conducted to enhance the performance and applicability of ADP. In [30], an integral model predictive control strategy based on decentralized online system identification was proposed, which is applied to voltage and frequency regulation in microgrids. In [31], the ADP method was employed to address the infinite-horizon optimal control problem for sliding mode dynamics, and a model-free decentralized sliding mode control scheme was designed for each subsystem. In [32], an optimization criterion was established based on zero-sum differential game theory, and a decentralized zero-sum differential game strategy was derived using data-driven methods to stabilize LSS. However, the majority of these studies focus on systems with moderate complexity or centralized architectures, with limited exploration in LSS characterized by high-dimensional states and distributed control structures [33]. The application of ADP in the decentralized control of LSS presents a promising avenue for research with significant theoretical and practical implications.

As mentioned above, despite some advancements in decentralized control and resilient strategies for LSS, existing approaches often face limitations in addressing the combined challenges of DoS attacks and incomplete system information. To bridge these gaps, this paper proposes a novel data-driven decentralized resilient control framework under DoS attacks, and the main contributions of this work are as follows:

1) Distinct from existing studies in [34], [35], and [36], this work investigates a broader class of LSS that are simultaneously subject to DoS attacks and unknown dynamic uncertainties. A key novelty lies in the utilization of online data to design optimal controllers without requiring complete knowledge of system dynamics.
2) By integrating data-driven techniques into decentralized control frameworks, the proposed method achieves robust disturbance attenuation and resilience against DoS attacks. This integration enhances the scalability and adaptability of the control strategy, especially in complex and uncertain environments.
3) A novel two-stage ADP algorithm is developed to approximate optimal decentralized control policies under incomplete system knowledge and stochastic disturbances. The algorithm is computationally efficient and capable of ensuring both stability and resilience in the presence of DoS attacks.

II. Problem Formulation

The dynamics of the ith subsystem within the LSS can be described by the following state-space representation:

$$\dot{x}_i(t) = A_i x_i(t) + B_i u_i(t) + D_i(f_i(y,t) + \omega_i(x_i,t)) \quad (1)$$

$$y_i(t) = C_i x_i(t), \quad i = 1, 2, \ldots, N \quad (2)$$

where $x_i(t) \in \mathbb{R}^{n_i}$ denotes the state vector of subsystem i; $u_i(t) \in \mathbb{R}^{m_i}$ represents the local control input; $y_i(t) \in \mathbb{R}^{p_i}$ is the measured output; $f_i(y,t) \in \mathbb{R}^{q_i}$ captures the interdependencies among subsystems, representing interactions or external inputs derived from the system outputs $y(t)$ with $y = [y_1^{\mathrm{T}}, y_2^{\mathrm{T}}, \ldots, y_N^{\mathrm{T}}]^{\mathrm{T}}$; $\omega_i(x_i,t) \in \mathbb{R}^{q_i}$ is the unknown matched uncertainty and is piecewise continuous in t. $A_i \in \mathbb{R}^{n_i \times n_i}$, $B_i \in \mathbb{R}^{n_i \times m_i}$, $C_i \in \mathbb{R}^{p_i \times n_i}$, and $D_i \in \mathbb{R}^{n_i \times q_i}$ are system matrices.

The effect of DoS attacks on the control input can be modeled as follows:

$$\bar{u}_i(t) = \mu_i(t) u_i(t) \quad (3)$$

where $\bar{u}_i(t)$ represents the actual control input received by subsystem i, and $u_i(t)$ is the intended control input generated by the controller. The binary variable $\mu_i(t)$ is a Bernoulli random variable with $E\{\mu_i(t)\} = \bar{\mu}_i$ that models the occurrence of DoS attacks. Specifically, $\mu_i(t) = 1$ indicates that the control signal is successfully transmitted to the subsystem, while $\mu_i(t) = 0$ represents a DoS attack, during which the control signal is blocked or lost.

Remark 1: This formulation explicitly captures the stochastic nature of DoS attacks, which occur randomly over time and interrupt the transmission of control signals within the

LSS. By incorporating the Bernoulli random variable $\mu_i(t)$ into the system model, the adverse impact of these attacks on the system dynamics and stability can be rigorously characterized. Specifically, the random and intermittent behavior of $\mu_i(t)$ provides a realistic representation of communication vulnerabilities that may arise from adversarial actions or unexpected network failures.

Remark 2: Many existing control methods [34], [35] either assume ideal communication conditions or rely on known system models, which limits their effectiveness in the presence of unpredictable DoS events and unknown uncertainties. In contrast, our proposed framework directly integrates the stochastic DoS model into the control design process, enabling resilient performance even under frequent and randomly occurring communication interruptions. This modeling approach forms the foundation for developing robust and adaptive control strategies that safeguard system stability and performance in adversarial environments.

Based on (3), the dynamics of each subsystem i subject to DoS attacks can be described by

$$\dot{x}_i(t) = A_i x_i(t) + B_i \bar{u}_i(t) + D_i(f_i(y,t) + \omega_i(x_i,t)). \tag{4}$$

To maintain generality, let us assume that $\text{rank}(B_i) = b_i \leq m_i$. According to linear algebra principles, there exists a nonsingular transformation matrix $M_i \in \mathbb{R}^{n_i \times n_i}$ such that $M_i B_i = [0_{m_i \times (n_i - b_i)}, B_{i2}^{\mathrm{T}}]^{\mathrm{T}}$, where $B_{i2} \in \mathbb{R}^{b_i \times m_i}$ has full row rank. For simplicity, we assume that B_i is already in this form. Consequently, the ith subsystem described in (1) and (2) can be reformulated as follows:

$$\begin{aligned}\dot{x}_{i1}(t) &= A_{i11}x_{i1}(t) + A_{i12}x_{i2}(t) \\ &\quad + D_{i1}(f_i(y,t) + \omega_i(x_{i1},t)) \qquad (5)\\ \dot{x}_{i2}(t) &= A_{i21}x_{i1}(t) + A_{i22}x_{i2}(t) + B_{i2}\bar{u}_i(t) \\ &\quad + D_{i2}(f_i(y,t) + \omega_i(x_{i2},t)) \qquad (6)\\ y_i(t) &= C_{i1}x_{i1}(t) + C_{i2}x_{i2}(t) \qquad (7)\end{aligned}$$

where

$$x_i = \begin{bmatrix} x_{i1} \\ x_{i2} \end{bmatrix}, \quad A_i = \begin{bmatrix} A_{i11} & A_{i12} \\ A_{i21} & A_{i22} \end{bmatrix}, \quad B_i = \begin{bmatrix} 0 \\ B_{i2} \end{bmatrix},$$
$$C_i = \begin{bmatrix} C_{i1} & C_{i2} \end{bmatrix}, \quad D_i = \begin{bmatrix} D_{i1}^{\mathrm{T}} & D_{i2}^{\mathrm{T}} \end{bmatrix}^{\mathrm{T}}.$$

Control Objective: The objective of this paper is to design a decentralized controller for each subsystem of the LSS that ensures resilient performance in the presence of DoS attacks and unknown dynamic uncertainties. Specifically, the proposed controller is expected to fulfill the following requirements:

1) For each subsystem $i = 1, 2, \ldots, N$, the closed-loop signals in (5)–(7) must remain uniformly bounded over time. Furthermore, the overall LSS, described by equations (1) and (2), should exhibit global asymptotic stability, despite the presence of network-induced disturbances and partial knowledge of the system dynamics.
2) The decentralized controller must effectively attenuate disturbances in each subsystem despite random DoS attacks and unknown uncertainties, while meeting a predefined performance criterion.

To facilitate the complete design of the control scheme, the following assumptions are introduced.

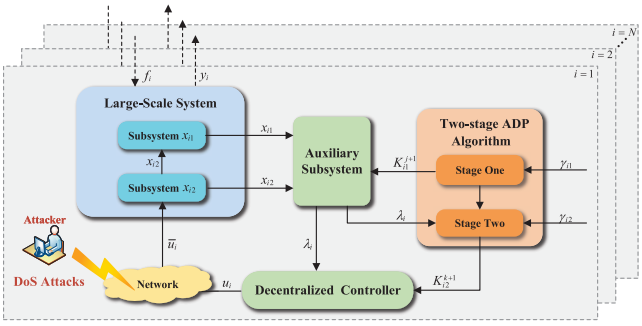

Fig. 1. Schematic of the decentralized control for LSS under DoS attacks.

Assumption 1: The matched uncertainty function $\omega_i(x_i,t)$ is locally Lipschitz continuous in $x_i(t)$, satisfying the following inequality:

$$\|\omega_i(x_i,t)\| \leq \alpha_i \|x_i(t)\| \tag{8}$$

where $\alpha_i \geq 0$ is an unknown constant.

Assumption 2: The interconnection function $f_i(y,t)$ is piecewise continuous with respect to t and locally Lipschitz continuous in $y(t)$, satisfying the following inequality:

$$\|f_i(y,t)\| \leq \zeta_i \|y(t)\| \tag{9}$$

where $\zeta_i > 0$ is a known constant.

III. Optimal Decentralized Controller Design

Fig.1 illustrates the schematic of decentralized control for LSS under DoS attacks. For the control problem of the ith subsystem (5)-(7), the H_∞ control approach is employed to optimize the control performance under external disturbances. This problem is equivalent to solving a zero-sum game, where the control input $u_i(t)$ minimizes the performance index while the disturbance ω_i maximizes it. To facilitate the optimization, the variable x_{i2} is introduced as a virtual control input of the subsystem (5). Then, the performance index is defined as:

$$J_{i1}(x_{i1}, x_{i2}, \tilde{\omega}_{i1}) = \int_0^\infty \left(x_{i1}^{\mathrm{T}} Q_{i1} x_{i1} + x_{i2}^{\mathrm{T}} R_{i1} x_{i2} - \gamma_{i1}^2 \tilde{\omega}_{i1}^{\mathrm{T}} \tilde{\omega}_{i1} \right) \mathrm{d}t \tag{10}$$

where $\tilde{\omega}_{i1}(t) = f_i(y,t) + \omega_i(x_{i1},t)$, Q_{i1} and R_{i1} are positive definite matrices, $\gamma_{i1} > 0$ is a prescribed disturbance attenuation level.

In optimal control theory, it is well established that the performance index J_{i1} is minimized by the optimal control input $x_{i2}^* = -K_{i1}^* x_{i1}$ and the worst disturbance $\tilde{\omega}_{i1}^* = L_{i1}^* x_{i1}$, where the feedback control gain K_{i1}^* and the disturbance policy gain L_{i1}^* is given by

$$K_{i1}^* = R_{i1}^{-1} A_{i12}^{\mathrm{T}} P_{i1}^*, \tag{11}$$
$$L_{i1}^* = \gamma_{i1}^{-2} D_{i1}^{\mathrm{T}} P_{i1}^*. \tag{12}$$

Here, P_{i1}^* denotes the unique positive definite solution to the following algebraic Riccati equation (ARE):

$$\begin{aligned} P_{i1}A_{i11} + A_{i11}^{\mathrm{T}} P_{i1} - P_{i1}A_{i12}R_{i1}^{-1}A_{i12}^{\mathrm{T}}P_{i2} \\ + \gamma_{i1}^{-2} P_{i1} D_{i1} D_{i1}^{\mathrm{T}} P_{i1} + Q_{i1} = 0. \end{aligned} \tag{13}$$

Directly obtaining an analytical solution is generally infeasible, especially for high-dimensional systems or systems with intricate matrix structures. To address this, this paper provides an efficient ADP algorithm to approximate the numerical solution of the ARE, enabling practical implementation of optimal control strategies.

Define the auxiliary variable

$$\lambda_i(t) = x_{i2}(t) + K_{i1}x_{i1}(t). \tag{14}$$

Then, the subsystem (6) can be rewritten as

$$\dot{\lambda}_i(t) = \bar{A}_{i21}x_{i1}(t) + \bar{A}_{i22}\lambda_i(t) + B_{i2}\bar{u}_i(t) + \bar{D}_{i2}\tilde{\omega}_{i2}(t) \tag{15}$$

where

$$\begin{aligned}
\bar{A}_{i21} &= A_{i21} + K_{i1}A_{i11} - \big(A_{i22} + K_{i1}A_{i12}\big)K_{i1},\\
\bar{A}_{i22} &= A_{i22} + K_{i1}A_{i12}, \quad \bar{D}_{i2} = D_{i2} + K_{i1}D_{i1},\\
\tilde{\omega}_{i2}(t) &= f_i(y,t) + \bar{D}_{i2}^{-1}\big(K_{i1}D_{i1}\omega_i(x_{i1},t) + D_{i2}\omega_i(x_{i2},t)\big).
\end{aligned}$$

Denote the performance index for the subsystem (15):

$$\begin{aligned}
&J_{i2}(\lambda_i, u_i, \tilde{\omega}_{i2})\\
&= \int_0^\infty \Big(\lambda_i^{\mathrm{T}}Q_{i2}\lambda_i + u_i^{\mathrm{T}}R_{i2}u_i - \gamma_{i2}^2\tilde{\omega}_{i2}^{\mathrm{T}}\tilde{\omega}_{i2}\Big)\mathrm{d}t
\end{aligned} \tag{16}$$

where $\gamma_{i2} > 0$ denotes the disturbance attenuation level of subsystem (15), matrices Q_{i2} and R_{i2} are positive definite.

Similar to (11)-(12), the optimal control input u_i^* and the worst disturbance response $\tilde{\omega}_{i2}^*$ are determined as:

$$u_i^* = -R_{i2}^{-1}B_{i2}^{\mathrm{T}}P_{i2}^*\lambda_i = -K_{i2}^*\lambda_i \tag{17}$$

$$\tilde{\omega}_{i2}^* = \gamma_{i2}^{-2}\bar{D}_{i2}^{\mathrm{T}}P_{i2}^*\lambda_i = L_{i2}^*\lambda_i \tag{18}$$

where K_{i2}^* and L_{i2}^* are the optimal control gain and the worst disturbance gain of subsystem (15), respectively. Meanwhile, positive definite matrix P_{i2}^* is the unique solution to the ARE:

$$\begin{aligned}
&P_{i2}\bar{A}_{i22} + \bar{A}_{i22}^{\mathrm{T}}P_{i2} - P_{i2}B_{i2}R_{i2}^{-1}B_{i2}^{\mathrm{T}}P_{i2}\\
&\qquad + \gamma_{i2}^{-2}P_{i2}\bar{D}_{i2}\bar{D}_{i2}^{\mathrm{T}}P_{i2} + Q_{i2} = 0.
\end{aligned} \tag{19}$$

Remark 3: Based on the optimal control theory, the matrix P can be derived by solving the ARE, which characterizes the relationship between the value function and the system dynamics. By substituting the value function into the Hamilton–Jacobi–Bellman (HJB) equation and applying the principle of optimality, an ARE can be established for P. This equation incorporates system matrices, weighting matrices for state and control inputs, and any disturbance attenuation terms, resulting in a closed-form relationship for P. Solving this equation yields the optimal state-feedback gains, ensuring that the control law minimizes the cost function while maintaining stability and performance for the system.

Combine (14) and (5), one can get

$$\dot{x}_{i1}(t) = \bar{A}_{i11}x_{i1}(t) + A_{i12}\lambda_i(t) + D_{i1}\tilde{\omega}_{i1}(t) \tag{20}$$

where $\bar{A}_{i11} = A_{i11} - A_{i12}K_{i1}$.

From (13) and (20), we have

$$\begin{aligned}
&P_{i1}\bar{A}_{i11} + \bar{A}_{i11}^{\mathrm{T}}P_{i1} - P_{i1}A_{i12}R_{i1}^{-1}A_{i12}^{\mathrm{T}}P_{i2}\\
&\qquad + \gamma_{i1}^{-2}P_{i1}D_{i1}D_{i1}^{\mathrm{T}}P_{i1} + Q_{i1} = 0.
\end{aligned} \tag{21}$$

Based on (15) and (20), the augmented ith subsystem is given by

$$\dot{\bar{x}}_i(t) = \bar{A}_i\bar{x}_i(t) + B_i\bar{u}_i + \bar{D}_i\tilde{\omega}_i(t) \tag{22}$$

$$y_i(t) = \bar{C}_{i1}x_{i1}(t) + C_{i2}\lambda_i(t) \tag{23}$$

where

$$\begin{aligned}
&\bar{x}_i(t) = \begin{bmatrix} x_{i1}(t)\\ \lambda_i(t)\end{bmatrix},\ \bar{A}_i = \begin{bmatrix} \bar{A}_{i11} & A_{i12}\\ \bar{A}_{i21} & \bar{A}_{i22}\end{bmatrix},\ \tilde{\omega}_i(t) = \begin{bmatrix}\tilde{\omega}_{i1}(t)\\ \tilde{\omega}_{i2}(t)\end{bmatrix},\\
&\bar{C}_{i1} = C_{i1} - C_{i2}K_{i1},\ \bar{D}_i = \mathrm{diag}\{D_{i,1}, \bar{D}_{i2}\}.
\end{aligned}$$

IV. Decentralized Stabilization of the Large-Scale System

In this section, we give the stability analysis for augmented subsystem (22) and (23) under the control policy u_i^*.

Theorem 1: Given the optimal control input u_i^* and the prescribed disturbance attenuation levels γ_{i1}, γ_{i2}, the states of the augmented subsystem (22) is uniformly bounded, and the states of the LSS in (1) and (2) are globally asymptotically stable, if there exists positive scalars α_i, β_i, ζ_i, η_i, ϱ_i, $\epsilon_{ij}(j = 1, 2, 3, 4)$, and positive definite matrices Q_{i1}, Q_{i2}, R_{i1}, R_{i2} such that

$$\begin{aligned}
&Q_{i1} \geq \big(\varrho_i + \epsilon_{i3}\big)I + \beta_i(1+\eta_i)\bar{C}_{i1}^{\mathrm{T}}\bar{C}_{i1},\\
&Q_{i2} \geq \big(\varrho_i + \epsilon_{i1}\big)I + \beta_i\Big(1 + \eta_i^{-1}\Big)C_{i2}^{\mathrm{T}}C_{i2},\\
&R_{i1} \leq \epsilon_{i1}I, \quad R_{i2} \leq \epsilon_{i3}(2\bar{\mu}_i - 1)B_{i2}^{\mathrm{T}}\big(\bar{A}_{i21}\bar{A}_{i21}^{\mathrm{T}}\big)^{-1}B_{i2},\\
&\epsilon_{i2} \geq 2\gamma_{i1}^2, \quad \epsilon_{i4} \geq 2\gamma_{i2}^2, \quad \varrho_i \geq \bar{\epsilon}_i\alpha_i, \quad \bar{\beta} \geq \bar{\zeta}.
\end{aligned}$$

where $\bar{\epsilon}_i = \max\{\epsilon_{i2}, \epsilon_{i4}\}$, $\bar{\beta} = \max_{1\leq i\leq N}\{\beta_i\}$, and $\bar{\zeta} = \sum_{i=1}^N \bar{\epsilon}_i\zeta_i$.

Proof: Choose the Lyapunov function as

$$V_i(\bar{x}_i) = E\Big\{x_{i1}^{\mathrm{T}}P_{i1}^*x_{i1} + \lambda_i^{\mathrm{T}}P_{i2}^*\lambda_i\Big\}. \tag{24}$$

Taking the derivative of V_i along the solutions to augmented subsystem (22), one has

$$\begin{aligned}
\dot{V}_i = {}& x_{i1}^{\mathrm{T}}\Big(P_{i1}^*A_{i11} + A_{i11}^{\mathrm{T}}P_{i1}^*\Big)x_{i1} - 2x_{i1}^{\mathrm{T}}P_{i1}^*A_{i12}K_{i1}^*x_{i1}\\
&+ 2x_{i1}^{\mathrm{T}}P_{i1}^*A_{i12}\lambda_i + 2x_{i1}^{\mathrm{T}}P_{i1}^*D_{i1}\tilde{\omega}_{i1}\\
&+ \lambda_i^{\mathrm{T}}\Big(P_{i2}^*\bar{A}_{i22} + \bar{A}_{i22}^{\mathrm{T}}P_{i2}^*\Big)\lambda_i + 2\lambda_i^{\mathrm{T}}P_{i2}^*\bar{A}_{i21}x_{i1}\\
&+ 2\bar{\mu}_i\lambda_i^{\mathrm{T}}P_{i2}^*B_{i2}u_i^* + 2\lambda_i^{\mathrm{T}}P_{i2}^*\bar{D}_{i2}\tilde{\omega}_{i2}.
\end{aligned} \tag{25}$$

Substituting (13) and (19) into (25) yields

$$\begin{aligned}
\dot{V}_i = {}& x_{i1}^{\mathrm{T}}\Big(P_{i1}^*A_{i12}R_{i1}^{-1}A_{i12}^{\mathrm{T}}P_{i2}^* - \gamma_{i1}^{-2}P_{i1}^*D_{i1}D_{i1}^{\mathrm{T}}P_{i1}^* - Q_{i1}\Big)x_{i1}\\
&-2x_{i1}^{\mathrm{T}}P_{i1}^*A_{i12}K_{i1}^*x_{i1}\\
&+ 2x_{i1}^{\mathrm{T}}P_{i1}^*A_{i12}\lambda_i + 2x_{i1}^{\mathrm{T}}P_{i1}^*D_{i1}\tilde{\omega}_{i1}\\
&+ \lambda_i^{\mathrm{T}}\Big(P_{i2}^*B_{i2}R_{i2}^{-1}B_{i2}^{\mathrm{T}}P_{i2}^* - \gamma_{i2}^{-2}P_{i2}^*\bar{D}_{i2}\bar{D}_{i2}^{\mathrm{T}}P_{i2}^* - Q_{i2}\Big)\lambda_i\\
&+2\lambda_i^{\mathrm{T}}P_{i2}^*\bar{A}_{i21}x_{i1}\\
&+ 2\bar{\mu}_i\lambda_i^{\mathrm{T}}P_{i2}^*B_{i2}u_i^* + 2\lambda_i^{\mathrm{T}}P_{i2}^*\bar{D}_{i2}\tilde{\omega}_{i2}.
\end{aligned} \tag{26}$$

From (11) and (17), it follows that

$$\begin{aligned}
\dot{V}_i = {}& \bar{x}_i^{\mathrm{T}}\bar{Q}_i\bar{x}_i - \gamma_{i1}^{-2}x_{i1}^{\mathrm{T}}P_{i1}^*D_{i1}D_{i1}^{\mathrm{T}}P_{i1}^*x_{i1}\\
&- x_{i1}^{\mathrm{T}}P_{i1}^*A_{i12}R_{i1}^{-1}A_{i12}^{\mathrm{T}}P_{i1}^*x_{i1} + 2x_{i1}^{\mathrm{T}}P_{i1}^*A_{i12}\lambda_i
\end{aligned}$$

$$+2x_{i1}^{\mathrm{T}}P_{i1}^{*}D_{i1}\tilde{\omega}_{i1}-\gamma_{i2}^{-2}\lambda_i^{\mathrm{T}}P_{i2}\bar{D}_{i2}\bar{D}_{i2}^{\mathrm{T}}P_{i2}\lambda_i+2\lambda_i^{\mathrm{T}}P_{i2}^{*}\bar{A}_{i21}x_{i1}+2\lambda_i^{\mathrm{T}}P_{i2}^{*}\bar{D}_{i2}\tilde{\omega}_{i2}-(2\bar{\mu}_i-1)\lambda_i^{\mathrm{T}}P_{i2}^{*}B_{i2}R_{i2}^{-1}B_{i2}^{\mathrm{T}}P_{i2}^{*}\lambda_i \tag{27}$$

where $\bar{Q}_i=\mathrm{diag}\{-Q_{i1},-Q_{i2}\}$.

By completing the squares, one has

$$2x_{i1}^{\mathrm{T}}P_{i1}^{*}A_{i12}\lambda_i \le \epsilon_{i1}^{-1}x_{i1}^{\mathrm{T}}P_{i1}^{*}A_{i12}A_{i12}^{\mathrm{T}}P_{i1}^{*}x_{i1}+\epsilon_{i1}\lambda_i^{\mathrm{T}}\lambda_i, \tag{28}$$

$$2x_{i1}^{\mathrm{T}}P_{i1}^{*}D_{i1}\tilde{\omega}_{i1} \le 2\epsilon_{i2}^{-1}x_{i1}^{\mathrm{T}}P_{i1}^{*}D_{i1}D_{i1}^{\mathrm{T}}P_{i1}^{*}x_{i1}+\frac{1}{2}\epsilon_{i2}\tilde{\omega}_{i1}^{\mathrm{T}}\tilde{\omega}_{i1}, \tag{29}$$

$$2\lambda_i^{\mathrm{T}}P_{i2}^{*}\bar{A}_{i21}x_{i1} \le \epsilon_{i3}x_{i1}^{\mathrm{T}}x_{i1}+\epsilon_{i3}^{-1}\lambda_i^{\mathrm{T}}P_{i2}^{*}\bar{A}_{i21}\bar{A}_{i21}^{\mathrm{T}}P_{i2}^{*}\lambda_i, \tag{30}$$

$$2\lambda_i^{\mathrm{T}}P_{i2}^{*}\bar{D}_{i2}\tilde{\omega}_{i2} \le 2\epsilon_{i4}^{-1}\lambda_i^{\mathrm{T}}P_{i2}^{*}\bar{D}_{i2}\bar{D}_{i2}^{\mathrm{T}}P_{i2}^{*}\lambda_i+\frac{1}{2}\epsilon_{i4}\tilde{\omega}_{i2}^{\mathrm{T}}\tilde{\omega}_{i2}. \tag{31}$$

Substituting (28)-(31) into (27) yields

$$\begin{aligned}\dot{V}_i \le{}& \bar{x}_i^{\mathrm{T}}\Theta_i\bar{x}_i-\left(\gamma_{i1}^{-2}-2\epsilon_{i2}^{-1}\right)x_{i1}^{\mathrm{T}}P_{i1}^{*}D_{i1}D_{i1}^{\mathrm{T}}P_{i1}^{*}x_{i1}\\&-x_{i1}^{\mathrm{T}}P_{i1}^{*}A_{i12}\left(R_{i1}^{-1}-\epsilon_{i1}^{-1}I\right)A_{i12}^{\mathrm{T}}P_{i1}^{*}x_{i1}\\&-\left(\gamma_{i2}^{-2}-2\epsilon_{i4}^{-1}\right)\lambda_i^{\mathrm{T}}P_{i2}\bar{D}_{i2}\bar{D}_{i2}^{\mathrm{T}}P_{i2}\lambda_i-\lambda_i^{\mathrm{T}}P_{i2}^{*}\\&\times\left((2\bar{\mu}_i-1)B_{i2}R_{i2}^{-1}B_{i2}^{\mathrm{T}}-\epsilon_{i3}^{-1}\bar{A}_{i21}\bar{A}_{i21}^{\mathrm{T}}\right)P_{i2}^{*}\lambda_i\\&+\frac{1}{2}\epsilon_{i2}\tilde{\omega}_{i1}^{\mathrm{T}}\tilde{\omega}_{i1}+\frac{1}{2}\epsilon_{i4}\tilde{\omega}_{i2}^{\mathrm{T}}\tilde{\omega}_{i2}\end{aligned} \tag{32}$$

where $\Theta_i=\mathrm{diag}\{\epsilon_{i3}I-Q_{i1},\epsilon_{i1}I-Q_{i2}\}$.

By using the similar method in [37], we get

$$\begin{aligned}\dot{V}_i \le{}& \bar{x}_i^{\mathrm{T}}\bar{\Theta}_i\bar{x}_i-\varrho_i x_{i1}^{\mathrm{T}}x_{i1}-\varrho_i\lambda_i^{\mathrm{T}}\lambda_i\\&-\left(\gamma_{i1}^{-2}-2\epsilon_{i2}^{-1}\right)x_{i1}^{\mathrm{T}}P_{i1}^{*}D_{i1}D_{i1}^{\mathrm{T}}P_{i1}^{*}x_{i1}\\&-x_{i1}^{\mathrm{T}}P_{i1}^{*}A_{i12}\left(R_{i1}^{-1}-\epsilon_{i1}^{-1}I\right)A_{i12}^{\mathrm{T}}P_{i1}^{*}x_{i1}\\&-\left(\gamma_{i2}^{-2}-2\epsilon_{i4}^{-1}\right)\lambda_i^{\mathrm{T}}P_{i2}\bar{D}_{i2}\bar{D}_{i2}^{\mathrm{T}}P_{i2}\lambda_i-\lambda_i^{\mathrm{T}}P_{i2}^{*}\\&\times\left((2\bar{\mu}_i-1)B_{i2}R_{i2}^{-1}B_{i2}^{\mathrm{T}}-\epsilon_{i3}^{-1}\bar{A}_{i21}\bar{A}_{i21}^{\mathrm{T}}\right)P_{i2}^{*}\lambda_i\\&+\frac{1}{2}\epsilon_{i2}\tilde{\omega}_{i1}^{\mathrm{T}}\tilde{\omega}_{i1}+\frac{1}{2}\epsilon_{i4}\tilde{\omega}_{i2}^{\mathrm{T}}\tilde{\omega}_{i2}-\beta_i y_i^{\mathrm{T}}y_i\end{aligned} \tag{33}$$

where $\bar{\Theta}_i=\mathrm{diag}\{\bar{\Theta}_{i1},\bar{\Theta}_{i2}\}$, $\bar{\Theta}_{i1}=(\varrho_i+\epsilon_{i3})I+\beta_i(1+\eta_i)\bar{C}_{i1}^{\mathrm{T}}\bar{C}_{i1}-Q_{i1}$, $\bar{\Theta}_{i2}=(\varrho_i+\epsilon_{i1})I+\beta_i(1+\eta_i^{-1})C_{i2}^{\mathrm{T}}C_{i2}-Q_{i2}$.

From the conditions in Theorem 1, it leads to

$$\dot{V}_i \le -\varrho_i\|\bar{x}_i\|^2-\beta_i\|y_i\|^2+\bar{\epsilon}_i\|\tilde{\omega}_i\|^2. \tag{34}$$

From Assumption 1 and 2, it can be derived that

$$\dot{V}_i \le -(\varrho_i-\bar{\epsilon}_i\alpha_i)\|\bar{x}_i\|^2-\beta_i\|y_i\|^2+\bar{\epsilon}_i\zeta_i\|y\|^2. \tag{35}$$

Similar to the approach in [38], we obtain

$$\sum_{i=1}^{N}\dot{V}_i(\bar{x}_i) \le -\sum_{i=1}^{N}(\varrho_i-\bar{\epsilon}_i\alpha_i)\|\bar{x}_i\|^2-\left(\bar{\beta}-\bar{\zeta}\right)\|y\|^2. \tag{36}$$

This completes the proof.

V. Two-Stage ADP Algorithm for the Large-Scale System

Although (11) and (17) establishes the theoretical foundation for deriving the optimal control policy, its implementation relies on accurate knowledge of system matrices, which may not always be available in practical scenarios. To address this limitation, this section introduces a novel decentralized ADP algorithm tailored to approximate the optimal control input u_i^* under conditions of incomplete system information. The proposed algorithm adopts a two stage design: in the first stage, auxiliary matrices P_{i1}^{j} and K_{i1}^{j} are iteratively updated to approximate their optimal counterparts P_{i1}^{*} and K_{i1}^{*}; in the second stage, these results are further leveraged to construct P_{i2}^{k} and K_{i2}^{k}, which serve as approximations for the optimal matrices P_{i2}^{*} and K_{i2}^{*}, respectively.

A. Stage-One of ADP

For the purpose of solving (21), it follows from (20) that

$$\begin{aligned}\frac{\mathrm{d}}{\mathrm{d}t}\left(x_{i1}^{\mathrm{T}}P_{i1}x_{i1}\right)={}& x_{i1}^{\mathrm{T}}\left(P_{i1}\bar{A}_{i11}+\bar{A}_{i11}^{\mathrm{T}}P_{i1}\right)x_{i1}\\&+2\left(x_{i2}+K_{i1}x_{i1}\right)^{\mathrm{T}}A_{i12}^{\mathrm{T}}P_{i1}x_{i1}+2\tilde{\omega}_{i1}^{\mathrm{T}}D_{i1}^{\mathrm{T}}P_{i1}x_{i1}.\end{aligned} \tag{37}$$

Substituting (21) into (37) yields

$$\begin{aligned}\frac{\mathrm{d}}{\mathrm{d}t}\left(x_{i1}^{\mathrm{T}}P_{i1}x_{i1}\right)={}& x_{i1}^{\mathrm{T}}\left(P_{i1}A_{i12}R_{i1}^{-1}A_{i12}^{\mathrm{T}}P_{i2}-\gamma_{i1}^{-2}P_{i1}\right.\\&\left.\times D_{i1}D_{i1}^{\mathrm{T}}P_{i1}-Q_{i1}\right)x_{i1}+2\tilde{\omega}_{i1}^{\mathrm{T}}D_{i1}^{\mathrm{T}}P_{i1}x_{i1}\\&+2\left(x_{i2}+K_{i1}x_{i1}\right)^{\mathrm{T}}A_{i12}^{\mathrm{T}}P_{i1}x_{i1}.\end{aligned} \tag{38}$$

Then, it follow from (11), (12) and (38) that

$$\begin{aligned}\frac{\mathrm{d}}{\mathrm{d}t}\left(x_{i1}^{\mathrm{T}}P_{i1}x_{i1}\right)={}& x_{i1}^{\mathrm{T}}\left(K_{i1}^{\mathrm{T}}R_{i1}K_{i1}-\gamma_{i1}^{2}L_{i1}^{\mathrm{T}}L_{i1}-Q_{i1}\right)x_{i1}\\&+2\left(x_{i2}+K_{i1}x_{i1}\right)^{\mathrm{T}}R_{i1}K_{i1}x_{i1}+2\gamma_{i1}^{2}x_{i1}^{\mathrm{T}}L_{i1}^{\mathrm{T}}L_{i1}x_{i1}.\end{aligned} \tag{39}$$

Integrating on both sides of (39), we have

$$\begin{aligned}x_{i1}^{\mathrm{T}}P_{i1}x_{i1}\big|_{t}^{t+\tau_r}={}& \int_{t}^{\tau_r}x_{i1}^{\mathrm{T}}\tilde{Q}_{i1}x_{i1}\mathrm{d}s\\&+2\int_{t}^{t+\tau_r}\left(x_{i2}+K_{i1}x_{i1}\right)^{\mathrm{T}}R_{i1}K_{i1}x_{i1}\mathrm{d}s\\&+2\gamma_{i1}^{2}\int_{t}^{t+\tau_r}x_{i1}^{\mathrm{T}}L_{i1}^{\mathrm{T}}L_{i1}x_{i1}\mathrm{d}s\end{aligned} \tag{40}$$

where $\tilde{Q}_{i1}=K_{i1}^{\mathrm{T}}R_{i1}K_{i1}-\gamma_{i1}^{2}L_{i1}^{\mathrm{T}}L_{i1}-Q_{i1}$.

Using Kronecker product representation, we have

$$x_{i1}^{\mathrm{T}}\tilde{Q}_{i1}x_{i1}=\left(x_{i1}^{\mathrm{T}}\otimes x_{i1}^{\mathrm{T}}\right)\mathrm{vec}\left(\tilde{Q}_{i1}\right), \tag{41}$$

$$\begin{aligned}&\left(x_{i2}+K_{i1}x_{i1}\right)^{\mathrm{T}}R_{i1}K_{i1}x_{i1}\\&=\left(x_{i1}^{\mathrm{T}}\otimes x_{i2}^{\mathrm{T}}+x_{i1}^{\mathrm{T}}\otimes\left(x_{i1}^{\mathrm{T}}K_{i1}^{\mathrm{T}}\right)\right)(I\otimes R_{i1})\mathrm{vec}(K_{i1})\\&=\left(\left(x_{i1}^{\mathrm{T}}\otimes x_{i2}^{\mathrm{T}}\right)(I\otimes R_{i1})\right.\\&\quad\left.+\left(x_{i1}^{\mathrm{T}}\otimes x_{i1}^{\mathrm{T}}\right)\left(I\otimes\left(K_{i1}^{\mathrm{T}}R_{i1}\right)\right)\right)\mathrm{vec}(K_{i1}),\end{aligned} \tag{42}$$

$$x_{i1}^{\mathrm{T}}L_{i1}^{\mathrm{T}}L_{i1}x_{i1}=\left(x_{i1}^{\mathrm{T}}\otimes x_{i1}^{\mathrm{T}}\right)\left(I\otimes L_{i1}^{\mathrm{T}}\right)\mathrm{vec}(L_{i1}). \tag{43}$$

To simplify expression, define

$$\Pi_i(z_1,z_2)=\Big[z_1\otimes z_2\big|_t^{t+\tau_1},\, z_1\otimes z_2\big|_{t+\tau_1}^{t+\tau_2},\, \ldots,\, z_1\otimes z_2\big|_{t+\tau_{r-1}}^{t+\tau_r}\Big]^{\mathrm{T}},$$

$$\Lambda_i(z_1,z_2)=\Big[\int_t^{t+\tau_1} z_1\otimes z_2\mathrm{d}s,\, \int_{t+\tau_1}^{t+\tau_2} z_1\otimes z_2\mathrm{d}s,\, \ldots,\, \int_{t+\tau_{r-1}}^{t+\tau_r} z_1\otimes z_2\mathrm{d}s\Big]^{\mathrm{T}}$$

where $0<\tau_1<\tau_2<\cdots<\tau_r$ are known constants.

From (41)-(43), (40) can be rewritten as follows

$$\Omega_{i1}\begin{bmatrix}\mathrm{vec}\big(P_{i1}^{j+1}\big)\\ \mathrm{vec}\big(K_{i1}^{j+1}\big)\\ \mathrm{vec}\big(L_{i1}^{j+1}\big)\end{bmatrix}=\Psi_{i1} \tag{44}$$

where

$$\Omega_{i1}=\Big[\Pi_i(x_{i1},x_{i1}),\ -2\Lambda_i(x_{i1},x_{i2})(I\otimes R_{i1})\\ -2\Lambda_i(x_{i1},x_{i1})\big(I\otimes\big(\big(K_{i1}^{j}\big)^{\mathrm{T}}R_{i1}\big)\big),\\ -2\gamma_{i1}^2\Lambda_i(x_{i1},x_{i1})\big(I\otimes\big(L_{i1}^{j}\big)^{\mathrm{T}}\big)\Big],$$

$$\Psi_{i1}=\Lambda_i(x_{i1},x_{i1})\mathrm{vec}\big(\tilde{Q}_{i1}\big).$$

B. Stage-Two of ADP

Similar to (37), it follows from (15) that

$$\frac{\mathrm{d}}{\mathrm{d}t}\big(\lambda_i^{\mathrm{T}}P_{i2}\lambda_i\big)=\lambda_i^{\mathrm{T}}\big(P_{i2}\bar{A}_{i22}+\bar{A}_{i22}^{\mathrm{T}}P_{i2}\big)\lambda_i+2x_{i1}^{\mathrm{T}}\bar{A}_{i21}^{\mathrm{T}}P_{i2}\lambda_i\\ +2\bar{\mu}_i u_i^{\mathrm{T}}B_{i2}^{\mathrm{T}}P_{i2}\lambda_i+2\tilde{\omega}_{i2}^{\mathrm{T}}\bar{D}_{i2}^{\mathrm{T}}P_{i2}\lambda_i. \tag{45}$$

From (19) and (45), we have

$$\frac{\mathrm{d}}{\mathrm{d}t}\big(\lambda_i^{\mathrm{T}}P_{i2}\lambda_i\big)=\lambda_i^{\mathrm{T}}\big(P_{i2}B_{i2}R_{i2}^{-1}B_{i2}^{\mathrm{T}}P_{i2}-\gamma_{i2}^{-2}P_{i2}\bar{D}_{i2}\\ \times\bar{D}_{i2}^{\mathrm{T}}P_{i2}-Q_{i2}\big)\lambda_i+2x_{i1}^{\mathrm{T}}\bar{A}_{i21}^{\mathrm{T}}P_{i2}\lambda_i\\ +2\bar{\mu}_i u_i^{\mathrm{T}}B_{i2}^{\mathrm{T}}P_{i2}\lambda_i+2\tilde{\omega}_{i2}^{\mathrm{T}}\bar{D}_{i2}^{\mathrm{T}}P_{i2}\lambda_i. \tag{46}$$

Substituting (17) and (18) into (46) leads to

$$\frac{\mathrm{d}}{\mathrm{d}t}\big(\lambda_i^{\mathrm{T}}P_{i2}\lambda_i\big)=\lambda_i^{\mathrm{T}}\big(K_{i2}^{\mathrm{T}}R_{i2}K_{i2}-\gamma_{i2}^2L_{i2}^{\mathrm{T}}L_{i2}-Q_{i2}\big)\lambda_i\\ +2x_{i1}^{\mathrm{T}}\bar{A}_{i21}^{\mathrm{T}}P_{i2}\lambda_i+2\bar{\mu}_i\lambda_i^{\mathrm{T}}K_{i2}^{\mathrm{T}}R_{i2}K_{i2}\lambda_i\\ +2\gamma_{i2}^2\lambda_i^{\mathrm{T}}L_{i2}^{\mathrm{T}}L_{i2}\lambda_i. \tag{47}$$

Integrating on both sides of (47) yields

$$\lambda_i^{\mathrm{T}}P_{i2}\lambda_i\big|_t^{t+\tau_r}=\int_t^{t+\tau_r}\lambda_i^{\mathrm{T}}\tilde{Q}_{i2}\lambda_i\mathrm{d}s\\ +2\int_t^{t+\tau_r}x_{i1}^{\mathrm{T}}\bar{A}_{i21}^{\mathrm{T}}P_{i2}\lambda_i\mathrm{d}s+2\gamma_{i2}^2\int_t^{t+\tau_r}\lambda_i^{\mathrm{T}}L_{i2}^{\mathrm{T}}L_{i2}\lambda_i\mathrm{d}s\\ +2\bar{\mu}_i\int_t^{t+\tau_r}\lambda_i^{\mathrm{T}}K_{i2}^{\mathrm{T}}R_{i2}K_{i2}\lambda_i\mathrm{d}s \tag{48}$$

where $\tilde{Q}_{i2}=K_{i2}^{\mathrm{T}}R_{i2}K_{i2}-\gamma_{i2}^2L_{i2}^{\mathrm{T}}L_{i2}-Q_{i2}$.

By Kronecker product representation, one has

$$\lambda_i^{\mathrm{T}}\tilde{Q}_{i2}\lambda_i=(\lambda_i^{\mathrm{T}}\otimes\lambda_i^{\mathrm{T}})\mathrm{vec}\big(\tilde{Q}_{i2}\big), \tag{49}$$

$$x_{i1}^{\mathrm{T}}\bar{A}_{i21}^{\mathrm{T}}P_{i2}\lambda_i=(\lambda_i^{\mathrm{T}}\otimes x_{i1}^{\mathrm{T}})\mathrm{vec}\big(\bar{A}_{i21}^{\mathrm{T}}P_{i2}\big), \tag{50}$$

$$\lambda_i^{\mathrm{T}}K_{i2}^{\mathrm{T}}R_{i2}K_{i2}\lambda_i=(\lambda_i^{\mathrm{T}}\otimes\lambda_i^{\mathrm{T}})\big(I\otimes\big(K_{i2}^{\mathrm{T}}R_{i2}\big)\big)\mathrm{vec}\big(K_{i2}\big), \tag{51}$$

$$\lambda_i^{\mathrm{T}}L_{i2}^{\mathrm{T}}L_{i2}\lambda_i=(\lambda_i^{\mathrm{T}}\otimes\lambda_i^{\mathrm{T}})\big(I\otimes L_{i2}^{\mathrm{T}}\big)\mathrm{vec}(L_{i2}). \tag{52}$$

From (49)-(52), (48) can be rewritten as follows

$$\Omega_{2i}\begin{bmatrix}\mathrm{vec}\big(P_{i2}^{k+1}\big)\\ \mathrm{vec}\big(\bar{A}_{i21}^{\mathrm{T}}P_{i2}^{k+1}\big)\\ \mathrm{vec}\big(K_{i2}^{k+1}\big)\\ \mathrm{vec}\big(L_{i2}^{k+1}\big)\end{bmatrix}=\Psi_{2i} \tag{53}$$

where

$$\Omega_{2i}=\Big[\Pi_i(\lambda_i,\lambda_i),\ -2\Lambda_i(\lambda_i,x_{i1}),\ -2\bar{\mu}_i\Lambda_i(\lambda_i,\lambda_i)\\ \times\big(I\otimes\big(\big(K_{i2}^{k}\big)^{\mathrm{T}}R_{i2}\big)\big),\ -2\gamma_{i2}^2\Lambda_i(\lambda_i,\lambda_i)\big(I\otimes\big(L_{i2}^{k}\big)^{\mathrm{T}}\big)\Big],$$

$$\Psi_{2i}=\Lambda_i(\lambda_i,\lambda_i)\mathrm{vec}\big(\tilde{Q}_{i2}\big).$$

Algorithm 1: Two-Stage ADP Algorithm

Input: System states x_{i1} and x_{i2}, disturbance attenuation levels γ_{i1} and γ_{i2}, attacks parameter $\bar{\mu}_i$;
Output: Optimal control input u_i^*;
Step 1. Choose the appropriate matrices Q_{i1}, Q_{i2}, R_{i1}, and R_{i2} based on the Theorem 1.
Step 2. Solve for P_{i1}^{j+1}, K_{i1}^{j+1}, and L_{i1}^{j+1} using (44).
if $\|P_{i1}^{j+1}-P_{i1}^{j}\|\le\varphi_i$ **then**
  set $K_{i1}^*=K_{i1}^{j+1}$.
else
  set $j=j+1$, and return **Step 2**;
end
where φ_i is a sufficiently small constant.
Step 3. Calculate λ_i based on x_{i1}, x_{i2}, and K_{i1}^*.
Step 4. Solve for P_{i2}^{k+1}, K_{i2}^{k+1}, and L_{i2}^{k+1} using (53).
if $\|P_{i2}^{k+1}-P_{i2}^{k}\|\le\varphi_i$ **then**
  set $K_{i2}^*=K_{i2}^{k+1}$.
else
  set $k=k+1$, and return **Step 4**;
end
Step 5. Substituting K_{i2}^* into (17) to get the optimal control input u_i^*.

To tackle the challenges of decentralized control in LSS affected by unknown uncertainties and DoS attacks, we propose an ADP algorithm based on a two-stage iterative learning framework. The key idea is to update the control gains K_{i1} and K_{i2} through successive iterations until convergence is achieved. The detailed steps of the two-stage ADP algorithm are shown in the following Algorithm 1.

This iterative scheme guarantees convergence to an optimal control solution, even in the presence of uncertainties and DoS attacks. Its flexibility and robustness make it a practical approach for decentralized resilient control in LSS.

Remark 4: The convergence feasibility of the proposed two-stage ADP algorithm is supported by theoretical analysis, ensuring that the iterative procedure for obtaining the optimal control policy converges under specific conditions.

Following the methodology outlined in [37], the convergence of Algorithm 1 is ensured by satisfying certain rank conditions and preserving the stability properties of the closed-loop system. Specifically, if the system matrix is Hurwitz and the excitation condition is sufficiently met throughout the iteration process, the ARE solution P_{i1}^{*} and P_{i2}^{*} are guaranteed to asymptotically approach their respective optimal solutions. These conditions establish both the theoretical soundness and practical viability of the proposed algorithm in real-world decentralized control scenarios for LSS.

Remark 5: The proposed two-stage ADP algorithm is developed based on the decomposition of the LSS into two interconnected subsystems. Each subsystem independently performs policy iteration to learn its own local optimal control strategy. Compared with conventional ADP methods, the proposed two-stage framework improves scalability, accelerates convergence, and enhances robustness under communication constraints and system uncertainties. These properties make the algorithm particularly suitable for real-world large-scale applications such as multi-machine power systems and networked control environments.

VI. Simulation

In power systems, synchronous operation of all generators is essential to ensure stable and reliable performance. Under steady-state conditions, the system frequencies are equal, maintaining synchronization across generators. However, disturbances and DoS attacks can cause frequency deviations, leading to mechanical vibrations in the generators and disrupting the power output. These disruptions can adversely affect the normal operation of user equipment and the overall stability of the power grid.

To address these issue, this section focuses on applying the proposed control algorithm to achieve optimal control in a multimachine power system with $N = 10$ subsystems under dynamic conditions. By leveraging online learning techniques, the algorithm is designed to mitigate disturbances and attacks, ensuring that the system frequencies remain synchronized at the rated frequency. The ith subsystem is described by the following differential equations, which capture the dynamics of generator rotor angles, angular velocities, and mechanical and electrical power flows:

$$\dot{\delta}_i(t) = w_i(t) \tag{54}$$

$$\dot{w}_i(t) = -\frac{\mathcal{D}_i}{2H_i} w_i(t) + \frac{w_0}{2H_i}\left(P_i^m(t) - P_i^e(t)\right) \tag{55}$$

$$\dot{P}_i^m(t) = \frac{1}{T_i}\left(-P_i^m(t) + u_i^g(t)\right) \tag{56}$$

$$P_i^e(t) = E_{qi}\sum_{j=1}^{N} E_{qj}\left(\mathcal{B}_i \sin\delta_{ij}(t) + G_i \cos\delta_{ij}(t)\right) \tag{57}$$

where $\delta_i(t)$ and $w_i(t)$ are the rotor angle and angular velocity deviation of generator i, respectively; $P_i^m(t)$ and $P_i^e(t)$ are the mechanical and electrical power of generator i; $u_i^g(t)$ is the governor control input; H_i is the inertia constant; $\mathcal{D}_i$ is the damping coefficient; T_i is the governor time constant; w_0 is the synchronous angular velocity; and $\delta_{ij}(t) = \delta_i(t) - \delta_j(t)$ represents the angle difference between generators i and j. The terms E_{qi}, $\mathcal{B}_i$, and G_i are parameters related to the internal voltage and line characteristics of generator.

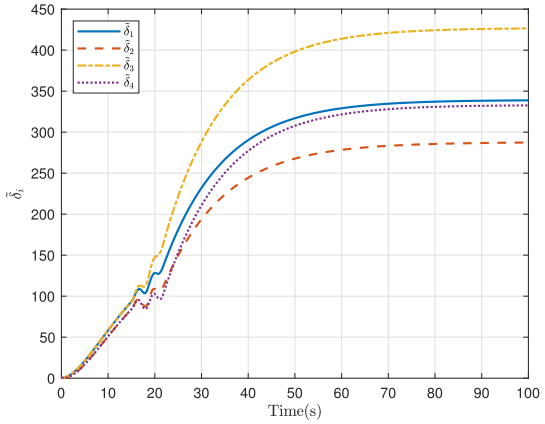

Fig. 2. State responses of rotor angle deviation $\tilde{\delta}_i$ of subsystems.

Similar to [39], the subsystem (54)–(57) can be rewritten as

$$\dot{\tilde{\delta}}_i(t) = w_i(t) \tag{58}$$

$$\dot{w}_i(t) = -\frac{\mathcal{D}_i}{2H_i} w_i(t) + \frac{w_0}{2H_i}\left(\tilde{P}_i^m(t) - F_i(t)\right) \tag{59}$$

$$\dot{\tilde{P}}_i^m(t) = \frac{1}{T_i}\left(-\tilde{P}_i^m(t) + u_i(t)\right) \tag{60}$$

$$F_i(t) = 2E_{qi}\sum_{j=1}^{N} E_{qj}\left(\mathcal{B}_i \cos\bar{\delta}_{ij}(t) - G_i \sin\bar{\delta}_{ij}(t)\right)\sin\hat{\delta}_{ij}(t)$$

where $\tilde{\delta}_i(t) = \delta_i(t) - \delta_{i0}$, $u_i(t) = u_i^g(t) - P_{i0}^e$, $\tilde{P}_i^m(t) = P_i^m(t) - P_{i0}^e$, $F_i(t) = P_i^e(t) - P_{i0}^e$, $\delta_{ij0} = \delta_{i0} - \delta_{j0}$, $\bar{\delta}_{ij}(t) = (\delta_{ij}(t) + \delta_{ij0})/2$, $\hat{\delta}_{ij}(t) = (\delta_{ij}(t) - \delta_{ij0})/2$, $P_{i0}^e = E_{qi}\sum_{j=1}^{N} E_{qj}(\mathcal{B}_i \sin\delta_{ij0} + G_i \cos\delta_{ij0})$.

Denote $x_{i1}(t) = [\tilde{\delta}_i(t), w_i(t)]^{\mathrm{T}}$, $x_{2i}(t) = \tilde{P}_i^m(t)$, and $f_i(y, t) = F_i(t)$. Then, (58)–(60) can be rewritten in the form of (5) and (6), where

$$A_{i11} = \begin{bmatrix} 0 & 1 \\ 0 & -\frac{\mathcal{D}_i}{2H_i} \end{bmatrix}, \quad A_{i12} = D_{i1} = \begin{bmatrix} 0 \\ -\frac{w_0}{2H_i} \end{bmatrix},$$

$$A_{i21} = [0, 0], \quad A_{i22} = -\frac{1}{T_i}, \; B_{i2} = \frac{1}{T_i}, \; D_{i2} = 0.$$

The detailed parameters of the 10-generator multimachine power system are adopted from [37]. The weight matrices are set to $Q_{i1} = \mathrm{diag}(5, 0.1)$, $Q_{i2} = 0.1$, $R_{i1} = 1$, and $R_{i2} = 100$. The disturbance attenuation levels are chosen as $\gamma_{i1} = 1$ and $\gamma_{i2} = 1$. The parameter for iteration termination is chosen as $\varphi_i = 0.01$. A severe disturbance with $\omega_i = 1.8\sin(0.2t)r(t)$ is applied during $15s < t < 22s$, while mild disturbances are present at other times, where $r(t)$ denotes a uniformly distributed random variable in the range $(0, 1)$. A subset of the initial conditions is assigned as $x_1(0) = [0.5, 0, -0.1]^T$, $x_2(0) = [0.5, -1, -0.1]^T$, $x_3(0) = [0.5, 0, -0.1]^T$, and $x_4(0) = [0.5, -1, -0.1]^T$, and the remaining settings are provided in [37].

Fig. 2 shows the state responses of rotor angle deviation $\tilde{\delta}_i$ across different subsystems. This indicates that the proposed control scheme effectively achieves rotor angle

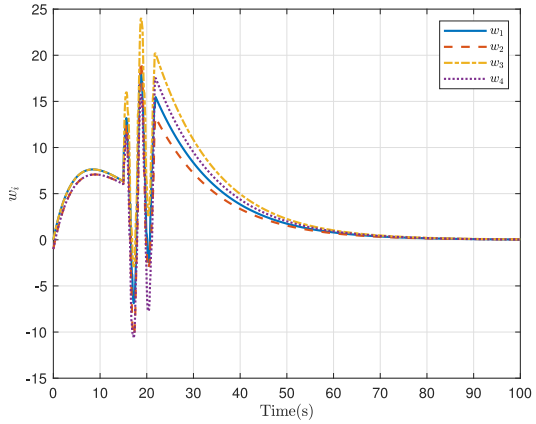

Fig. 3. State responses of angular velocity deviation w_i of subsystems.

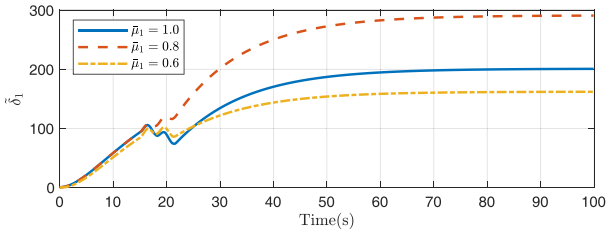

Fig. 4. Effect of DoS attacks intensity on rotor angle deviation $\tilde{\delta}_1$.

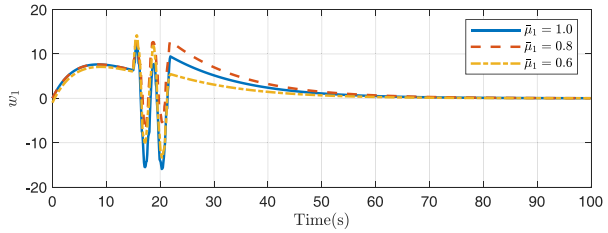

Fig. 5. Effect of DoS attacks intensity on angular velocity deviation w_1.

synchronization and ensures transient stability. Fig. 3 illustrates the angular velocity deviation w_i trajectories of each subsystem. This demonstrates the controller ability to stabilize frequency deviations, which is critical for the secure operation of power systems. Fig. 4 depicts the rotor angle deviation $\tilde{\delta}_1$ under DoS attacks with different intensities. As the attack strength increases, the system exhibits larger oscillations and slower convergence. Nevertheless, the state remains ultimately bounded, indicating the resilience of the proposed control method against communication disruptions. Fig. 5 presents the angular velocity deviation w_1 of under varying DoS attacks intensities. Although stronger attacks lead to greater overshoot and longer settling time, the system maintains overall stability, demonstrating the controller robustness under network disruptions.

Fig. 6 compares the rotor angle deviation $\tilde{\delta}_1$ under different control strategies in the absence of DoS attacks. Fig. 7 demonstrates the frequency response w_1 without DoS attacks under various control schemes. Fig. 8 shows the mechanical power deviation $\tilde{P}_1^m$ under different control strategies without DoS attacks. As shown in Figs. 6-8, the proposed two-stage ADP-based control method demonstrates the fastest convergence

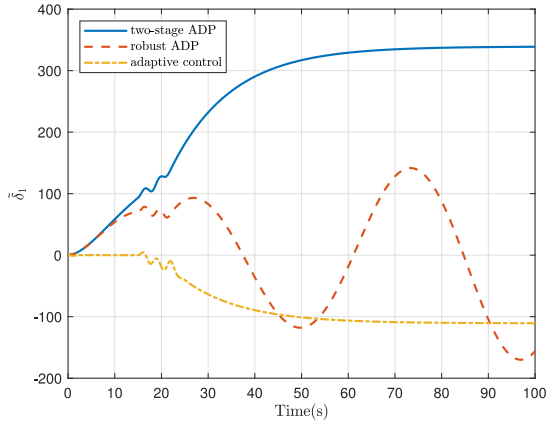

Fig. 6. Rotor angle deviation $\tilde{\delta}_1$ under different control strategies without DoS attacks.

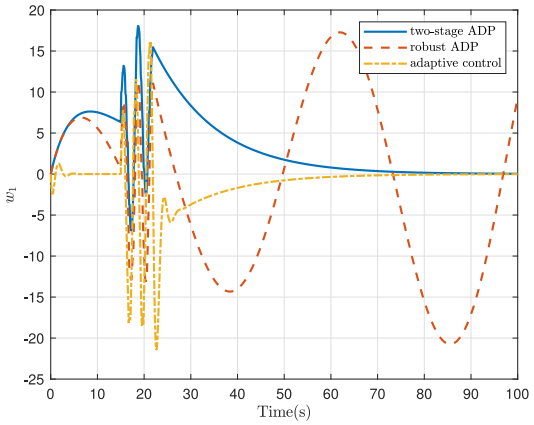

Fig. 7. Angular velocity deviation w_1 under different control strategies without DoS attacks.

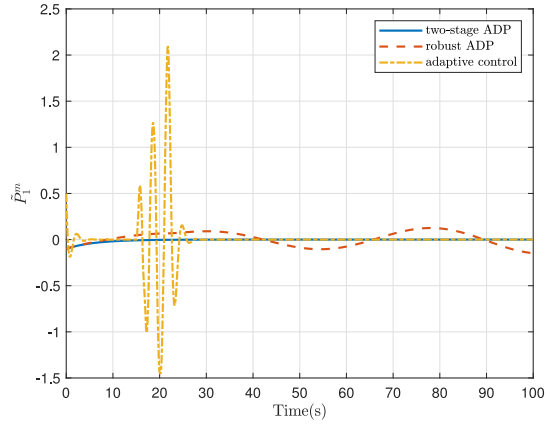

Fig. 8. Mechanical power deviation $\tilde{P}_1^m$ under different control strategies without DoS attacks.

rate and the smallest oscillation magnitude. Compared with the robust ADP-based control strategy in [38] and adaptive control method in [37], the proposed strategy provides superior transient performance and improved control accuracy.

Fig. 9 compares the rotor angle deviation $\tilde{\delta}_1$ under different control strategies in the presence of DoS attacks. Fig. 10 illustrates the angular velocity deviation w_1 under DoS attacks for various controllers. Fig. 11 presents the mechanical power

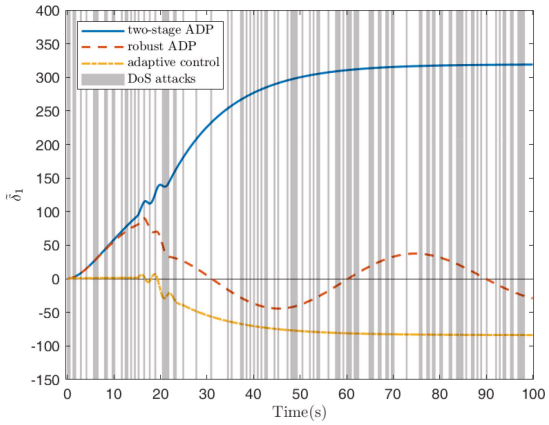

Fig. 9. Comparison of rotor angle deviation $\tilde{\delta}_1$ under different control strategies with DoS attacks.

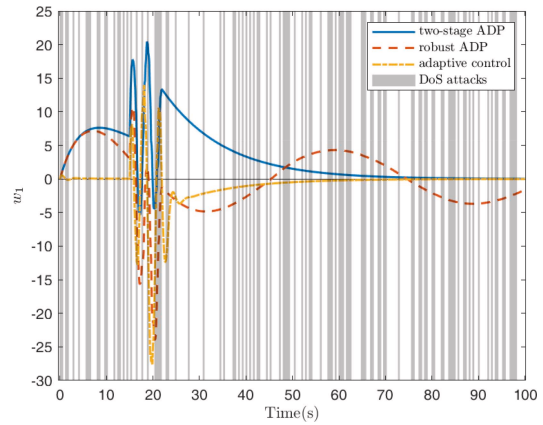

Fig. 10. Comparison of angular velocity deviation w_1 under different control strategies with DoS attacks.

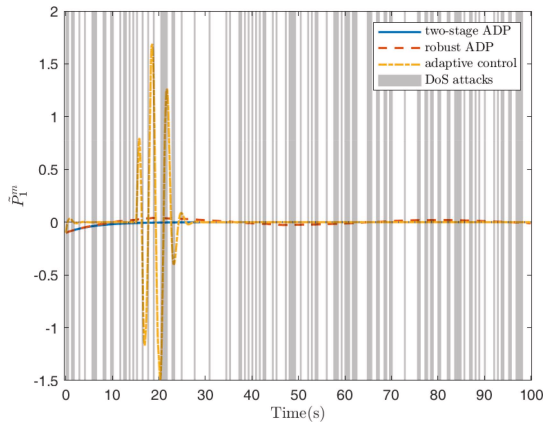

Fig. 11. Comparison of mechanical power deviation $\tilde{P}_1^m$ under different control strategies with DoS attacks.

deviation $\tilde{P}_1^m$ under DoS attacks. As illustrated in Figs. 9–11, the control methods from [37] and [38] exhibit larger oscillations and slower convergence under network disruption. In contrast, the proposed two-stage ADP-based control strategy achieves significantly improved stability and faster recovery, maintaining precise rotor angle regulation despite the presence of communication attacks.

TABLE I
COMPARISON OF w_1 UNDER DIFFERENT CONTROL STRATEGIES

Methods	Settling time	Overshooting	Steady-state error
two-stage ADP	72s	20.7129	0.0097
robust ADP	89s	24.2175	4.1568
adaptive control	78s	27.8547	0.0226

TABLE II
COMPARISON OF $\tilde{P}_1^m$ UNDER DIFFERENT CONTROL STRATEGIES

Methods	Settling time	Overshooting	Steady-state error
two-stage ADP	18s	0.1000	0.0039
robust ADP	36s	0.1000	0.0417
adaptive control	27s	1.6892	0.0073

Table I presents the control performance of different strategies for the angular velocity deviation w_1. The two-stage ADP method achieves a settling time of 72 seconds, which is 19.1% faster than the robust ADP and 7.7% faster than the adaptive control. In terms of overshooting, it reduces the peak value by 14.5% compared with robust ADP and by 25.6% compared with adaptive control. This improvement helps reduce mechanical stress and potential risk of instability during transient phases. These results highlight the practical advantages of the proposed method, such as faster recovery from disturbances, smoother transient behavior, and enhanced system resilience under challenging conditions.

Table II compares the control effect on the mechanical power deviation $\tilde{P}_1^m$. The two-stage ADP achieves a settling time of 18 seconds, representing a 50% improvement over the robust ADP and a 33.3% reduction compared to the adaptive control. It also yields the lowest steady-state error of 0.0039, marking a 46.6% decrease relative to the adaptive control. These results highlight the effectiveness of the proposed method in providing fast, accurate, and stable control, which helps reduce mechanical wear and improve system reliability under challenging conditions. In summary, the simulation results validate the effectiveness of the proposed two-stage ADP-based control strategy in attack scenarios.

VII. CONCLUSION

In this paper, a novel data-driven decentralized resilient control framework is proposed for LSS operating under DoS attacks. A two-stage ADP algorithm is developed to approximate the optimal control policy, even when system matrices are partially unknown. Compared to existing methods, the proposed approach achieves up to a 7.7% reduction in settling time and more than a 14.5% decrease in overshooting, demonstrating its superior performance in terms of convergence speed and disturbance rejection. For future research, key technical challenges include improving scalability to ultra-large networks, enhancing learning efficiency in real-time implementation, and ensuring robustness under various attacks.

REFERENCES

[1] J. Feng, B. Huang, X. Zhou, and X. Jin, "Large-scale multi-agent learning-based cloud-edge collaborative distributed PV data compression and information aggregation for multimodal network in power systems," *IEEE Trans. Consum. Electron.*, early access, Apr. 2, 2024, doi: 10.1109/TCE.2024.3384438.

[2] M. Kordestani, A. A. Safavi, and M. Saif, "Recent survey of large-scale systems: Architectures, controller strategies, and industrial applications," *IEEE Syst. J.*, vol. 15, no. 4, pp. 5440–5453, Dec. 2021.

[3] R. F. Araujo, L. A. B. Torres, and R. M. Palhares, "Plug-and-play distributed control of large-scale nonlinear systems," *IEEE Trans. Cybern.*, vol. 53, no. 4, pp. 2062–2073, Apr. 2023.

[4] L. Cao, Y. Pan, H. Liang, and C. K. Ahn, "Event-based adaptive neural network control for large-scale systems with nonconstant control gains and unknown measurement sensitivity," *IEEE Trans. Syst., Man, Cybern., Syst.*, vol. 54, no. 11, pp. 7027–7038, Nov. 2024.

[5] A. Papazafeiropoulos, J. An, P. Kourtessis, T. Ratnarajah, and S. Chatzinotas, "Achievable rate optimization for stacked intelligent Metasurface-assisted holographic MIMO communications," *IEEE Trans. Wireless Commun.*, vol. 23, no. 10, pp. 13173–13186, Oct. 2024.

[6] P. Verma, S. K. Sood, H. Kaur, M. Kumar, H. Wu, and S. S. Gill, "Data driven stochastic game network-based smart home monitoring system using IoT-enabled edge computing environments," *IEEE Trans. Consum. Electron.*, early access, Jun. 10, 2024, doi: 10.1109/TCE.2024.3411657.

[7] P. D. Paikrao et al., "Data driven neural speech enhancement for smart Healthcare in consumer electronics applications," *IEEE Trans. Consum. Electron.*, vol. 70, no. 2, pp. 4828–4838, May 2024.

[8] H. Guan, Q. Bai, and Q. Meng, "A decentralized signal-free intersection control framework for connected and autonomous vehicles," *IEEE Trans. Consum. Electron.*, early access, Jan. 8, 2025, doi: 10.1109/TCE.2025.3526938.

[9] J. Sun and Z. Zeng, "Predictor-based extended state observer for decentralized event-triggered control of large-scale systems with input and output delays," *IEEE Trans. Ind. Informat.*, vol. 20, no. 3, pp. 3913–3922, Mar. 2024.

[10] J. Liu, N. Zhang, L. Zha, X. Xie, and E. Tian, "Reinforcement learning-based decentralized control for networked interconnected systems with communication and control constraints," *IEEE Trans. Autom. Sci. Eng.*, vol. 21, no. 3, pp. 4674–4685, Jul. 2024.

[11] Y. Zhan, X. Li, and S. Tong, "Observer-based decentralized control for non-strict-feedback fractional-order nonlinear large-scale systems with unknown dead zones," *IEEE Trans. Neural Netw. Learn. Syst.*, vol. 34, no. 10, pp. 7479–7490, Oct. 2023.

[12] Q. Qu, H. Zhang, T. Feng, and H. Jiang, "Decentralized adaptive tracking control scheme for nonlinear large-scale interconnected systems via adaptive dynamic programming," *Neurocomputing*, vol. 225, pp. 1–10, Feb. 2017.

[13] C.-H. Xie and G.-H. Yang, "Decentralized adaptive fault-tolerant control for large-scale systems with external disturbances and actuator faults," *Automatica*, vol. 85, pp. 83–90, Nov. 2017.

[14] H. Wang, P. X. Liu, J. Bao, X.-J. Xie, and S. Li, "Adaptive neural output-feedback decentralized control for large-scale nonlinear systems with stochastic disturbances," *IEEE Trans. Neural Netw. Learn. Syst.*, vol. 31, no. 3, pp. 972–983, Mar. 2020.

[15] A. N. Jahromi, H. Karimipour, T. Halabi, Y. Zhu, and T. R. Gadekallu, "Multimodal game-theoretic cyber-attack projection in industrial control systems," *IEEE Trans. Consum. Electron.*, early access, Jul. 25, 2024, doi: 10.1109/TCE.2024.3433565.

[16] Y. Liu and Y. Chen, "Decentralized resilient finite-time-control for large-scale power systems via dynamic triggering against deception attacks," *IEEE Trans. Smart Grid*, vol. 14, no. 4, pp. 3210–3219, Jul. 2023.

[17] L. Zha, J. Miao, J. Liu, E. Tian, and C. Peng, "Privacy-preserving distributed estimation over sensor networks with multistrategy injection attacks: A chaotic encryption scheme," *IEEE Trans. Syst., Man, Cybern., Syst.*, early access, Apr. 25, 2025, doi: 10.1109/TSMC.2025.3560404.

[18] X. Li, N. Zhang, X. Xu, A.-T. Nguyen, K. Al-Haddad, and H. Zhang, "Attack-resilient event-triggered control of vehicle speed tracking system with DoS attacks: Experimental results," *IEEE Trans. Consum. Electron.*, vol. 70, no. 3, pp. 5079–5089, Aug. 2024.

[19] J. Zhao and G.-H. Yang, "Reinforcement-learning-based fuzzy adaptive finite-time optimal resilient control for large-scale nonlinear systems under false data injection attacks," *IEEE Trans. Fuzzy Syst.*, vol. 32, no. 4, pp. 2483–2495, Apr. 2024.

[20] W. Li, R. Ren, M. Shi, B. Lin, and K. Qin, "Seeking secure adaptive distributed discrete-time observer for networked agent systems under external Cyber attacks," *IEEE Trans. Consum. Electron.*, early access, Jan. 27, 2025, doi: 10.1109/TCE.2025.3535083.

[21] J. Liu, E. Gong, L. Zha, E. Tian, and X. Xie, "Interval type-2 fuzzy-model-based filtering for nonlinear systems with event-triggering weighted try-once-discard protocol and cyberattacks," *IEEE Trans. Fuzzy Syst.*, vol. 32, no. 3, pp. 721–732, Mar. 2024.

[22] D. Liu, B. Wang, K. Zhou, X. Cui, and K. Shi, "Distributed event-triggered collaborative control for multiagent systems against DoS attacks," *J. Franklin Inst.*, vol. 361, no. 11, p. 106959, 2024.

[23] L. Zha, J. Miao, J. Liu, E. Tian, and C. Peng, "Neural predictor-based formation control for unmanned surface vehicles under aperiodic DoS attacks: A noncooperative game approach," *IEEE Trans. Veh. Technol.*, early access, May 2, 2025, doi: 10.1109/TVT.2025.3566778.

[24] Y.-Y. Li and Y.-X. Li, "Adaptive decentralized fuzzy resilient control for large-scale nonlinear systems against stochastic disturbances and DoS attacks," *IEEE Trans. Fuzzy Syst.*, vol. 32, no. 3, pp. 1494–1503, Mar. 2024.

[25] F. Fang, J. Li, Y. Liu, and J. H. Park, "resilient control for multiagent systems with a sampled-data model against DoS attacks," *IEEE Trans. Ind. Informat.*, vol. 19, no. 1, pp. 780–789, Jan. 2023.

[26] S. Weng, D. Yue, J. Chen, and C. Dou, "Distributed resilient event-triggered control for power quality improvement in grid-tied microgrid under denial-of-service attack," *IEEE Syst. J.*, vol. 18, no. 2, pp. 860–871, Jun. 2024.

[27] W. Liu, J. Sun, G. Wang, F. Bullo, and J. Chen, "Data-driven self-triggered control via trajectory prediction," *IEEE Trans. Autom. Control*, vol. 68, no. 11, pp. 6951–6958, Nov. 2023.

[28] B. Li and Y. Yang, "Distributed fault detection for large-scale systems: A subspace-aided data-driven scheme with cloud-edge-end collaboration," *IEEE Trans. Ind. Informat.*, vol. 20, no. 10, pp. 12200–12209, Oct. 2024.

[29] F. Zhao, W. Gao, T. Liu, and Z.-P. Jiang, "Event-triggered robust adaptive dynamic programming with output feedback for large-scale systems," *IEEE Trans. Control Netw. Syst.*, vol. 10, no. 1, pp. 63–74, Mar. 2023.

[30] A. Ingalalli and S. Kamalasadan, "Data-driven decentralized online system identification-based integral model-predictive voltage and frequency control in microgrids," *IEEE Trans. Ind. Informat.*, vol. 20, no. 2, pp. 1963–1974, Feb. 2024.

[31] J. Song, L.-Y. Huang, H. R. Karimi, Y. Niu, and J. Zhou, "ADP-based security decentralized sliding mode control for partially unknown large-scale systems under injection attacks," *IEEE Trans. Circuits Syst. I, Reg. Papers*, vol. 67, no. 12, pp. 5290–5301, Dec. 2020.

[32] Y. Li, H. Zhang, Z. Wang, C. Huang, and H. Yan, "Decentralized control for large-scale systems with actuator faults and external disturbances: A data-driven method," *IEEE Trans. Neural Netw. Learn. Syst.*, vol. 35, no. 8, pp. 10882–10893, Aug. 2024.

[33] H. Wang, H. Luo, L. Ren, M. Huo, Y. Jiang, and O. Kaynak, "Data-driven design of distributed monitoring and optimization system for manufacturing systems," *IEEE Trans. Ind. Informat.*, vol. 20, no. 7, pp. 9455–9464, Jul. 2024.

[34] Y. Zhan and S. Tong, "Adaptive fuzzy output-feedback decentralized control for fractional-order nonlinear large-scale systems," *IEEE Trans. Cybern.*, vol. 52, no. 12, pp. 12795–12804, Dec. 2022.

[35] Z. Zhang, C. Yang, and S. S. Ge, "Decentralized adaptive control of large-scale nonlinear systems with time-delay interconnections and asymmetric dead-zone input," *IEEE Trans. Syst., Man, Cybern. Syst.*, vol. 53, no. 4, pp. 2259–2270, Apr. 2023.

[36] Y. Zhu and E. Fridman, "Observer-based decentralized predictor control for large-scale interconnected systems with large delays," *IEEE Trans. Autom. Control*, vol. 66, no. 6, pp. 2897–2904, Jun. 2021.

[37] T. Bian, Y. Jiang, and Z.-P. Jiang, "Decentralized adaptive optimal control of large-scale systems with application to power systems," *IEEE Trans. Ind. Electron.*, vol. 62, no. 4, pp. 2439–2447, Apr. 2015.

[38] Y. Jiang and Z.-P. Jiang, "Robust adaptive dynamic programming for large-scale systems with an application to multimachine power systems," *IEEE Trans. Circuits Syst. II, Exp. Briefs*, vol. 59, no. 10, pp. 693–697, Oct. 2012.

[39] G. Guo, Y. Wang, and D. Hill, "Nonlinear output stabilization control for multimachine power systems," *IEEE Trans. Circuits Syst. I, Fundam. Theory Appl.*, vol. 47, no. 1, pp. 46–53, Jan. 2000.

Lijuan Zha received the Ph.D. degree in control science and engineering from Donghua University, Shanghai, China, in 2018.

From 2017 to 2024, she was an Associate Professor with the College of Information Engineering, Nanjing University of Finance and Economics, Nanjing, China. From 2018 to 2023, she was a Postdoctoral Research Associate with the School of Mathematics, Southeast University, Nanjing. She is currently an Associate Professor with the College of Science, Nanjing Forestry University, Nanjing. Her current research interests include networked control systems, neural networks, and complex dynamical systems.

Jinzhao Miao received the B.S. and M.S. degrees in computer science and technology from the Nanjing University of Finance and Economics, Nanjing, China, in 2020 and 2025, respectively. He is currently pursuing the Ph.D. degree in computer science and technology with the School of Computer, Nanjing University of Information Science and Technology, Nanjing.

His research interests include networked control systems, unmanned systems, and neural networks.

Jinliang Liu (Senior Member, IEEE) received the Ph.D. degree in control theory and control engineering from the School of Information Science and Technology, Donghua University, Shanghai, China, in 2011.

He was a Postdoctoral Research Associate with the School of Automation, Southeast University, Nanjing, China, from December 2013 to June 2016. He was a Visiting Researcher/Scholar with the Department of Mechanical Engineering, University of Hong Kong, Hong Kong, from October 2016 to October 2017. He was a Visiting Scholar with the Department of Electrical Engineering, Yeungnam University, Gyeongsan, South Korea, from November 2017 to January 2018. From June 2011 to May 2023, he was an Associate Professor and then a Professor with the Nanjing University of Finance and Economics, Nanjing. In June 2023, he joined the Nanjing University of Information Science and Technology, Nanjing, where he is currently a Professor with the School of Computer Science. His research interests include networked control systems, complex dynamical networks, and time delay systems.

Engang Tian (Senior Member, IEEE) received the B.S. degree in mathematics from Shandong Normal University, Jinan, China, in 2002, the M.Sc. degree in operations research and cybernetics from Nanjing Normal University, Nanjing, China, in 2005, and the Ph.D. degree in control theory and control engineering from Donghua University, Shanghai, China, in 2008.

From 2011 to 2012, he was a Postdoctoral Research Fellow with the Hong Kong Polytechnic University, Hong Kong. From 2015 to 2016, he was a Visiting Scholar with the Department of Information Systems and Computing, Brunel University London, Uxbridge, U.K. From 2008 to 2018, he was an Associate Professor and then a Professor with the School of Electrical and Automation Engineering, Nanjing Normal University. In 2018, he was appointed as an Eastern Scholar by the Municipal Commission of Education, Shanghai, and joined the University of Shanghai for Science and Technology, Shanghai, where he is currently a Professor with the School of Optical-Electrical and Computer Engineering. He has published more than 100 papers in refereed international journals. His research interests include networked control systems, cyber attack, as well as nonlinear stochastic control and filtering.

Chen Peng (Senior Member, IEEE) received the B.S. and M.S. degrees in coal preparation, and the Ph.D. degree in control theory and control engineering from the Chinese University of Mining Technology, Xuzhou, China, in 1996, 1999, and 2002, respectively.

From September 2002 to August 2004, he was a Postdoctoral Research Fellow of Applied Math with Nanjing Normal University, Nanjing, China. From November 2004 to January 2005, he was a Research Associate with The University of Hong Kong, Hong Kong. From July 2006 to August 2007, he was a Visiting Scholar with the Queensland University of Technology, Brisbane, QLD, Australia. From September 2010 to August 2012, he was a Postdoctoral Research Fellow with Central Queensland University, Rockhampton, QLD, Australia. He is currently a Professor with the School of Mechatronic Engineering and Automation, Shanghai University, Shanghai, China. His current research interests include networked control systems, multiagent systems, power systems, and interconnected systems.

Dr. Peng was named a Highly Cited Researcher in 2020, 2021, and 2022 by Clarivate Analytics. He is an Associate Editor for a number of international journals, including the IEEE TRANSACTIONS ON INDUSTRIAL INFORMATICS, *Information Sciences*, and *Transactions of the Institute of Measurement and Control*.